Demonstration of Loop Reactor Operation

A. Y. Madai and M. Sheintuch
Dept. of Chemical Engineering, Technion-Israel Institute of Technology (IIT), Technion City, Haifa 32 000, Israel

DOI 10.1002/aic.11551
Published online July 9, 2008 in Wiley InterScience (www.interscience.wiley.com).

This article is the first experimental demonstration of autothermal operation in an open loop reactor for catalytic abatement of low-concentration volatile organic compounds (VOC). The system under investigation, which comprises three reactors organized in a loop with automatic switching of the feed position, has been successfully operated for ethylene oxidation. The influence of the feed flow rate and concentration on the pulse velocity and maximal temperature has been investigated. A simple analytical approximation for front velocity in the nonadiabatic one-dimensional (1D) model has been derived and compared with the experimental results. © 2008 American Institute of Chemical Engineers *AIChE J,* 54: 2413–2422, 2008
Keywords: catalytic, reactor design, autothermal reactor, combustion, chemical reactors, reaction engineering, forced unsteady-state reactors

Introduction

Several conceptual solutions that combine a packed bed and enthalpy recuperation have been suggested for abatement of low-concentration volatile organic compounds (VOC). These include the reverse-flow reactor (RF),[1,2] the loop or ring reactor (LR), which may take several forms as discussed below, the counter-current (CCR)[4] or the internal-recycle reactor and the reactor with external recycle and external heat exchanger. The loop reactor in the form composed of several units with feed switching between them has been simulated by Barresi and coworkers,[3] whereas we have generalized these results by studying the asymptotic solutions of loop reactors, in which a single exothermic reaction occurs.[4] Another form of a circulation loop reactor, in the form of single-port reactor in which a section near the inlet is heated via a heat-exchanger by the exit stream, was suggested by Gilles and Lauschke.[5]

This article is the first experimental verification of VOC combustion in an open loop reactor made of three catalytic reactors. The results are compared to a simple analytical approximation for front velocity in the nonadiabatic one-dimensional model.

We describe below the main features of reverse-flow and loop reactors. Flow-reversal reactors, in which the feed is varying between two ports, are currently attracting intensive research and have been applied commercially. The advantage of reactors with periodic flow reversal over simple once-through operation for attaining high temperatures has been demonstrated in many studies of adiabatic units during the past decade. This feature makes them especially attractive for VOC oxidation or NO reduction[1,2,6,7] (for a recent review, see Kolios et al.[8]). This high temperature results from the nature of heat loss in the two reactors: in a simple adiabatic fixed bed, the reaction heat is dissipated by convection, whereas in the flow-reversal unit with fast switching, heat is lost mainly by conduction, and this term can be mitigated by building long inert zones on both sides of the catalytic layer. The main advantage of a reactor with flow reversal for combustion purposes is that the bed temperature increases with the flow rate into the reactor, as more material is consumed. Other applications of this technology capitalized on the nonmonotonic temperature profile and were aimed at improving conversion of exothermic reversible equilibrium-limited reactions such as SO_2 oxidation[9,10] and methanol or ammonia synthesis.[11–13]

Correspondence concerning this article should be addressed to A. Y. Madai at amadai@tx.technion.ac.il or cermsll@technion.ac.il.

Table 1. Experiments Conditions

Parameter	Working Area
Velocity (m/s)	0.505–0.732
Residence time (s)	1.64–2.38
Ethylene concentration (% vol)	0.5–0.85
Switching (min)	62.8–533.7
Pressure (atm)	1–1.5

Open Loop reactors extend the two-port concept into feeding at several or many ports in several reactor units that are organized in a loop (Figure 1). To illustrate this concept, a loop reactor with N units ($N \geq 2$) is considered with a feed port and an exit port that are switched at every predetermined time interval σ. In the first interval, the feed flow enters the first reactor and exits from reactor N. This pattern will continue as long as the heat front is far from exiting reactor number one. At the second interval, the feed flow enters the second reactor and exits from the first reactor, and so on.

In the desired loop reactor operation, a temperature pulse (hot spot) is formed and rotates around the system. Its temperature can be increased significantly by pushing the pulse; the adiabatic temperature rise across a front in a fixed bed is known to increase with front velocity (v_{fr}) (and in turn with the fluid velocity, v_o) by a factor of $(v_o - v_{fr})/(v_o - \text{Le } v_{fr})$ compared with the stationary front ($v_{fr} = 0$). Some forms of periodic boundary conditions are required, of course, to sustain the periodic motion. Rotating pulses in a loop reactor may emerge provided that the switching velocity (v_{sw} i.e., unit length/switching time) and the pulse velocity are matched in a certain way. The maximal temperature in a loop reactor exceeds that in reverse flow reactor.[14]

The main drawback of the loop reactor is the narrow domain of switching velocities that support travelling pulses; the domain becomes narrower with decreasing ΔT_{ad} and forms a cusp shaped domain in the (ΔT_{ad}, v_{sw}) plane.[14] However, the maximal temperature in an adiabatic unit is obtained for Le $v_{sw}/v_o = 1$, which should be easy to maintain, if Le is known. Approximate boundaries of the domain of switching velocities where the pulse solution can be maintained were derived by Nekhamkina and Sheintuch (in press) for a first-order reaction. Because not all parameters (especially Le) are known exactly, we incorporate a control mechanism to sustain the pulse.

The article is structured as follows: the experimental apparatus and results are described in following two chapters. The mathematical model is presented in the following chapter along which the approximate solution derived for pulse velocity.

Experimental

A system made of three fixed bed reactors was arranged in the form of a loop (see Figures 1 and 2 for a flow chart and a schematic chart). We describe below the feed reactor, analysis, and control procedures. There are six control valves, which direct the flow in the system. To assure unidirectional flow in the system, three one-way valves have been constructed and placed at the exit of each reactor. These three stainless steel valves were constructed in a way that the flow is directed by a suspended ball, and they can withstand the high temperatures of the system. The other six valves were placed at the cold interface with the tubes outside the vacuum system.

The feed section includes the feed cylinders (ethylene gas, 99.9% purity from Gordon Gas and Chemicals) and compressed air, purification and drying systems, flow controllers, and a rotameter. The compressed air is passed through columns of silica gel and of activated carbon to remove traces of water and hydrocarbons. The system feed (ethylene) is controlled by a mass flow controller (Brooks) that was calibrated and adapted to the system. The air flow is measured by rotameter in a flow range of 10–50 l/min. The outlet CO_2 concentration is measured online by an infrared analyzer with a response time of 20 s (Emproco, Israel).

The three reactors are made of stainless steel (0.029-m diameter and 0.4-m long) and packed by spherical catalytic particles (0.5%, Pt/Al_2O_3 in 2–4-mm diameter, Johnson Matheys, England). The inert section (0.135-m long) was packed by similar size alumina pellet-shaped particles.

Fifteen thermocouples (type K) were placed along the three reactors and connected to an analog to digital signal convector. The data is displayed and stored in a PC in real time on the computer screen.

For startup purposes, the first reactor is wrapped by a cylindrical heating coil that enabled rapid heating. Following van de Beld (1997)[15] suggestion that the required temperature for full ethylene combustion catalyzed by Pt/Al_2O_3 (0.06%) is 136°C, the initial temperature imposed for the preheated unit in this research was 150°C. When the necessary temperature was achieved, under flow of air, the hydrocarbon was introduced into the system and the heating was turned off.

The three reactors are assembled inside a sealed cylinder (stainless steel 304) connected to a vacuum pump that creates a vacuum (0.7 torr) for the reduction of heat loss; this mechanism was used and studied in many works.[16,17] The inner wall of the cylinder is covered by an aluminum foil to reflect heat radiation from the system.

There are two simple methods for controlling the system:

1. Using constant time intervals predetermined at the beginning of the experiment. This approach is possible

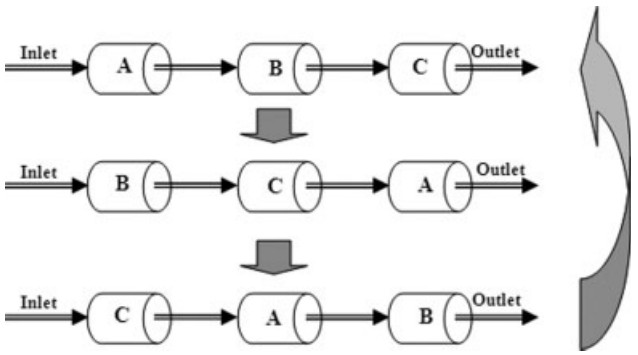

Figure 1. Scheme of the three-reactor loop system.

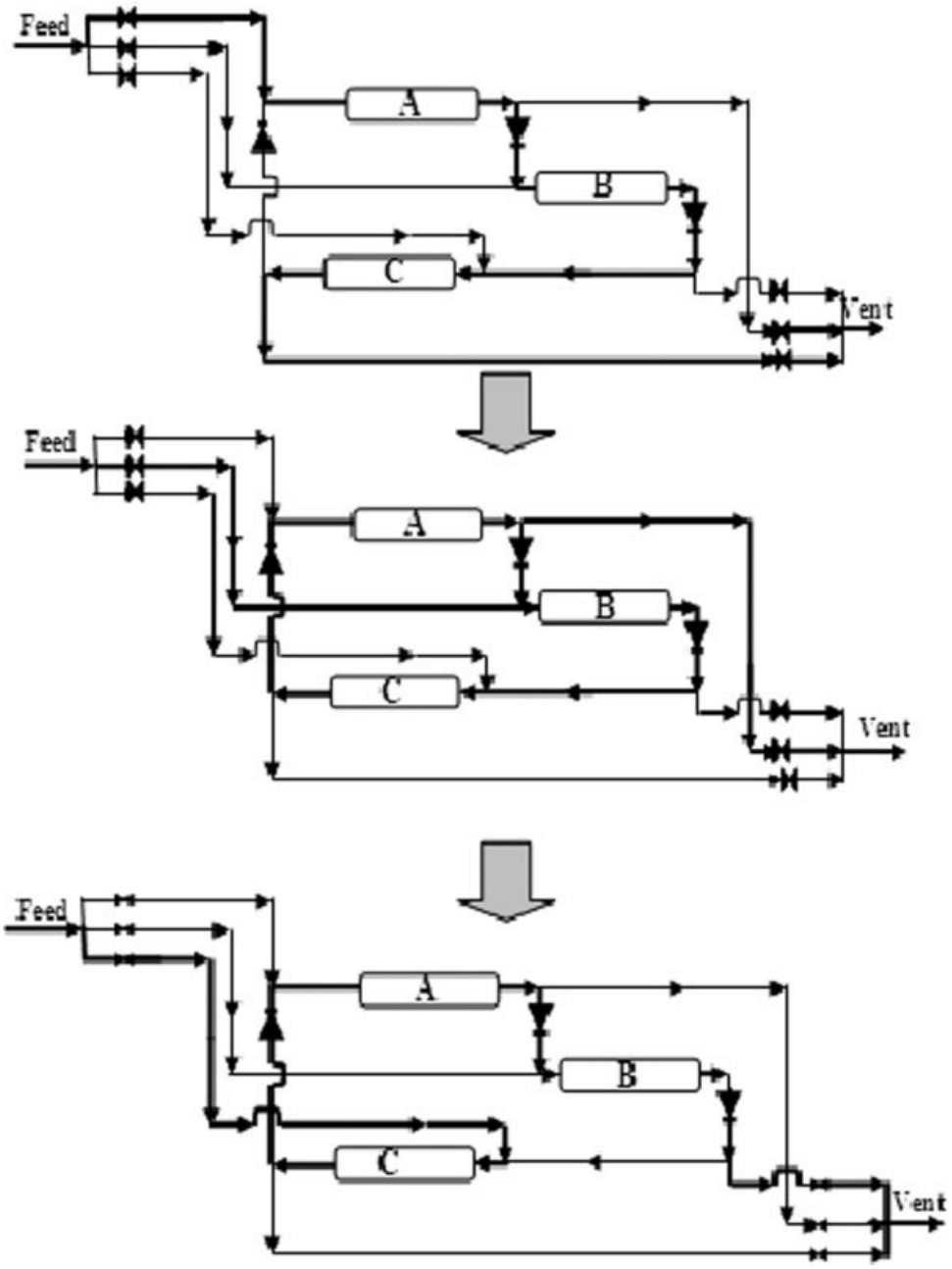

Figure 2. Valve arrangement in the loop reactor system.

when the parameters (especially heat capacity) are known exactly.

2. Using feedback control to regulate the switching as applied here: for two consecutive reactors, the feed is switched from one reactor to the following when the temperature measured at the entrance of the second reactor reaches T_{sw2} and the temperature at the entrance of the first reactor drops below T_{sw1}. This approach was suggested by Barresi and Fissore (2002)[18] and adopted here.

The reaction used in this work, the oxidation of ethylene on Pt/Al_2O_3,is characterized by high exotermicity and self-inhibition. Its rate was reported to exhibit negative-order kinetics with respect to ethylene at low temperature.[13] The rate expression reported by Mandler et al. (1983)[19] is

$$r_{\text{Ethylene}} = \frac{k'_{c_1c_2}}{(1+K_1c_1+K_2c_2)^2} = \frac{A'\exp(-\frac{E'}{RT})c_1c_2}{[1+A_1\exp(-\frac{E_1}{RT})c_1+A_2\exp(\frac{E_2}{RT})c_2]^2} \quad (1)$$

where C_1 and C_2 are ethylene and oxygen concentration in volume percentage. At high temperature, and with oxygen in excess, Eq. 1 is reduced to a simple first-order kinetics.

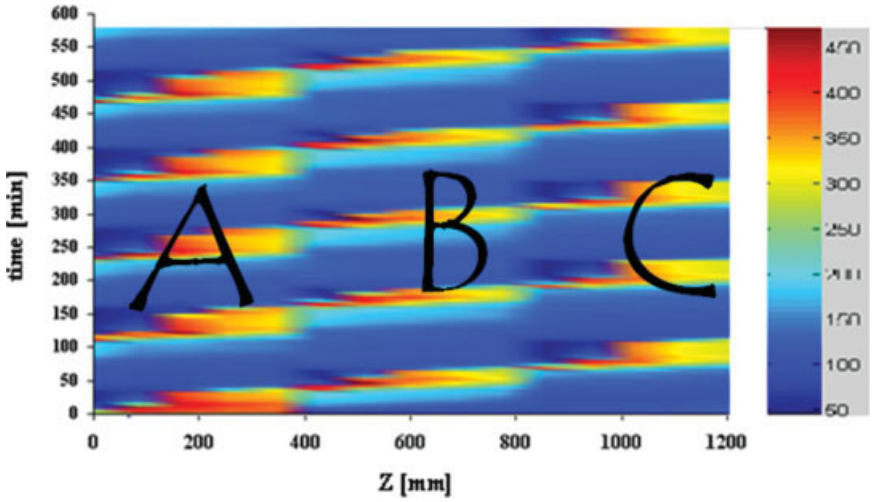

Figure 3. Spatio-temporal color-scaled temperature profile presented in the time-space plane (air flow 25 l/min or 0.63 m/s fluid velocity with 0.7% ethylene in the feed).

[Color figure can be viewed in the online issue, which is available at www.interscience.wiley.com.]

Experimental results

This is the first demonstration of the loop reactor system for exothermic VOC combustion. We report on the effect of varying feed flow rate and concentration (see Table 1). The switching cycle was determined by the first thermocouple at the entrance of the catalytic area in each reactor as explained above with $T_{sw1} \cong T_{ign} - 10^{\circ}C$ and $T_{sw2} \cong T_{ign} + 10^{\circ}C$. This control prevents the extinction of the system as well as from temperatures rising to an undesired level that may lead to deactivation.

Demonstration of loop-reactor system

A typical spatiotemporal temperature pattern of the system, shown by Figure 3 in a color-scale plot, exhibits a moving pulse pattern. These results were obtained after the reactor was initially heated up in air to 150°C (i.e., the ignition temperature of ethylene oxidation), and ethylene was subsequently added and the external heating stopped. Figure 4a demonstrated three temperature profiles (three snapshots) inside the closed loop system. Comparison of entire cycles after spatial translation shows overlapping temperature profiles (blue line and light blue line, Figure 4a). The pulse velocity obtained in this case was 1.75×10^{-4} m/s (slope of pattern in Figure 3).

The pulse speed matches the switching speed and depends mainly on the fluid velocity (v_o) and on the Lewis number (Le), the heat capacity ratio of the bed to the fluid. Theory shows that for an adiabatic system $v_{sw} \cong v_o/\mathrm{Le}$, yields the highest temperature. Note that Le is different in unit A due to the heating elements. The temperature profile repeats itself every 114 min (L/v_{sw}). In addition, it can be seen that the periodic steady state is attained only after two cycles (Figure 5b).

Flow velocity effect

One of the advantages of heat recuperating reactors (RFO, open loop) is that they become more efficient as feed flow rate increases. Theory shows that increasing the feed flow rate will increase the maximal temperature in an adiabatic unit.[3,4] Another minor effect, which leads to a temperature rise, is due to improvement of mass transfer effects at higher feed velocities. Experiments indeed show that increasing the feed flow rate leads to a linear rise of the maximal temperature in the system (Figure 5a, $v = 0.5$–0.7 m/s). Complete conversion was achieved in all cases. It can be also seen that the experimental results are in a good agreement with the analytical approximation we have developed (Eq. 13).

It is expected from the developed approximation that the pulse velocity should increase linearly with the feed velocity (Eqs. 10 and 12). The experimental results obtained within the narrow domain of flow rate studied follows well this prediction (Figure 5b).

Effect of contaminant concentration

An additional controllable parameter that can be changed independently is the contaminant (ethylene) concentration, which directly affects the adiabatic temperature rise (ΔT_{ab}). A high concentration of consumed reacted gas (C_{in}) is translated to additional energy. Figure 6 shows higher maximal temperatures (T_m) obtained in the experiments with increasing C_{in}. This behavior is also relatively well predicted by the analytical approximation (Figure 6) that also predicts a decline of the pulse velocity with increasing contaminant concentrations.

Mathematical model and analytical results

In this section, we derive an expression for the maximal temperature and pulse velocity in a nonadiabatic fixed bed, which are compared with experimental observations (Figures 5 and 6), assuming that the pulse in a loop reactor moves at the switching velocity. Although we are aware of approximate solution for front velocity in a nonadiabatic reactor,[20] we refer

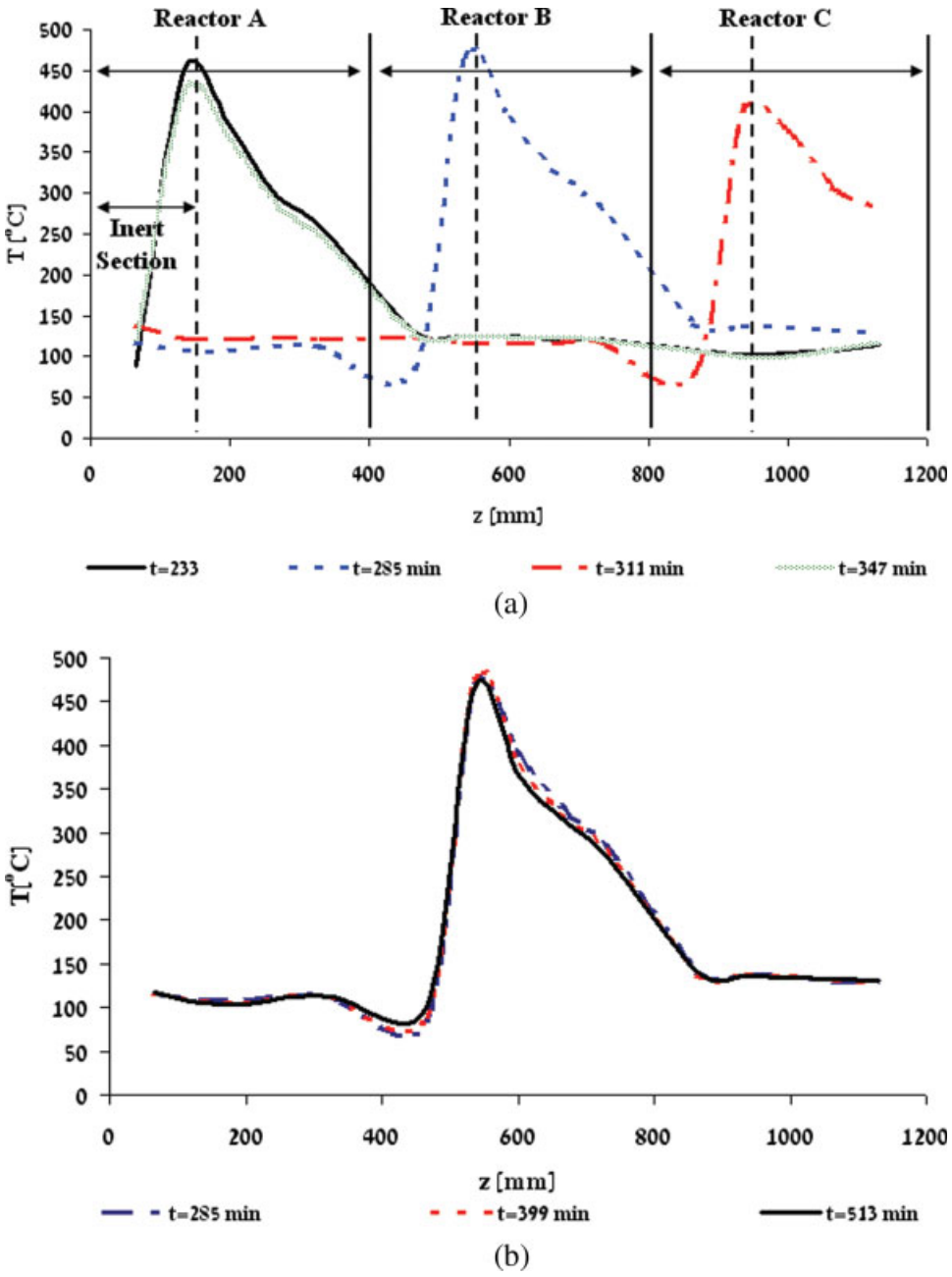

Figure 4. Three snapshots of the temperature pulse propagation (a) and their overlapping profiles (b) after spatial translation (conditions in as Figure 3).

[Color figure can be viewed in the online issue, which is available at www.interscience.wiley.com.]

to it at the end of this section and compare our results, showing that it cannot adequately describe our results.

Simulations show that the v_{fr} in an adiabatic long loop reactor is close to that in a once-through long reactor.[4] We derive the solution for nonadiabatic once-through reactor as an approximation for a bounded nonadiabatic loop reactor.

Consider a pseudohomogeneous one-dimensional (1D) model of a once-through nonadiabatic fixed bed reactor in which a reaction of a general kinetics occurs [$r(T, C)$ is the rate expression]. The enthalpy and mass balances are described by

$$(\rho c_p)_s(1-\varepsilon)\frac{\partial T}{\partial t} + (\rho c_p)_f v_o \frac{\partial T}{\partial z} - k_s \frac{\partial^2 T}{\partial z^2} = (-\Delta H)(1-\varepsilon) r(C,T) - \frac{4U}{d}(T - T_w) \quad (2)$$

$$\varepsilon \frac{\partial C}{\partial t} + v_o \frac{\partial C}{\partial z} - \varepsilon D \frac{\partial^2 C}{\partial z^2} = -(1-\varepsilon) r(C,T)$$

With appropriate initial and boundary (Danckwerts) conditions:

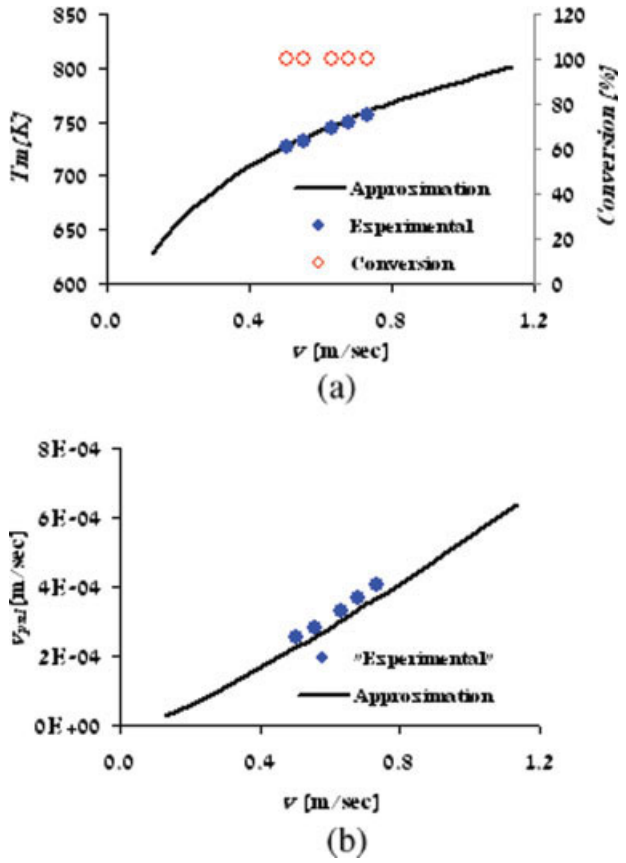

Figure 5. The dependence of the maximal measured temperature and conversion (a) and the measured pulse velocity (b) on fluid velocity (conditions in as Figure 4).

Also shown is their approximation by the model. [Color figure can be viewed in the online issue, which is available at www.interscience.wiley.com.]

$$
\begin{aligned}
&z = z_{\text{in}} \quad \varepsilon D\frac{\partial C}{\partial z} = v_{\text{o}}(C - c_{\text{in}}), \quad k_{\text{s}}\frac{\partial T}{\partial z} = (\rho C_{\text{p}})_{\text{f}} v_{\text{o}}(T - T_{\text{in}})\\
&z = z_{\text{out}} \quad \frac{\partial C}{\partial z} = \frac{\partial T}{\partial z} = 0\\
&t = 0 \quad C(z) = C_0; \quad T(z) = T_0
\end{aligned}
\tag{3}
$$

We limit our study to generic first-order activated and exothermic reactions with a rate of $r = A\exp(-E/R_{\text{g}}T)C$. To a first approximation, the conduction is const (k_{s}), axial dispersion of mass is assumed to be negligible[21] ($D \to 0$), and thermodynamic parameters (ρ, C_{p}) are assumed to be constant. With these assumptions, the system (Eqs. 3 and 4) may be rewritten in the dimensionless form as

$$
\begin{aligned}
&\text{Le}\frac{\partial y}{\partial \tau} + \frac{\partial y}{\partial \xi} - \frac{1}{P_{\text{e}_y}}\frac{\partial^2 y}{\partial \xi} = BDaR - W(y - y_{\text{w}});\\
&\frac{\partial x}{\partial \tau} + \frac{\partial x}{\partial \xi} = DaR\\
&R(x,y) = (1-x)\exp\left(\frac{\gamma y}{\gamma + y}\right);
\end{aligned}
\tag{4}
$$

$$
\begin{aligned}
&\tau = 0 : y(0,z) = y_0, \quad x(0,z) = x_0\\
&\xi = \xi_{\text{in}} \quad \frac{1}{P_{\text{e}_y}}\frac{\partial y}{\partial \xi} = y, \quad x = 0\\
&\xi = \xi_{\text{out}} \quad \frac{\partial y}{\partial \xi} = 0, \quad \frac{\partial x}{\partial \xi} = 0
\end{aligned}
\tag{5}
$$

With

$$
\begin{aligned}
&x = 1 - \frac{C}{C_{\text{in}}}, \quad y = \gamma\frac{T - T_{\text{in}}}{T_{\text{in}}}, \quad \xi = \frac{z}{L}, \quad \tau = \frac{tu}{\varepsilon L},\\
&y = \frac{E_{\text{a}}}{R_{\text{g}}T_{\text{in}}}, \quad B = \gamma\frac{(-\Delta H)C_0}{(\rho C_{\text{p}})_{\text{f}}T_{\text{in}}}, \quad Da = \frac{L(1-\varepsilon)A}{u}\exp(-\gamma),\\
&\text{Le} = \frac{(1-\varepsilon)(\rho C_{\text{p}})_{\text{s}}}{\varepsilon(\rho c P)_{\text{f}}}, \quad P_{\text{e}_y} = \frac{(\rho C_{\text{p}})_{\text{f}} uL}{k_{\text{s}}},\\
&W[U, L, d, (\rho C_{\text{p}})_{\text{f}}, v_{\text{o}}] = \frac{4UL}{d(\rho C_{\text{p}})_{\text{f}} v_{\text{o}}}
\end{aligned}
$$

To determine the propagation velocity and the maximal temperature, we assume the thermal front to be ideal, moving along an infinitely long bed at a constant velocity.[21] These conditions are met for an exothermic highly activated irreversible reaction, because a narrow reaction zone is formed (the reaction rate is negligible before and after the front). The corresponding asymptotic solution of the maximal temperature in a slow-switching finite-length loop reactor[14] was shown to approximately follow.

$$
F(y_{\text{m}}) = \frac{D_{\text{a}}}{P_{\text{e}_y}B}\left(1 + \frac{y_{\text{m}}}{\gamma}\right)^2 \exp\left(\frac{\gamma y_{\text{m}}}{\gamma + y_{\text{m}}}\right) = \frac{(1 - \varepsilon v_{\text{sw}}/v_{\text{o}})^2}{1 + \alpha(v_{\text{sw}}, y_{\text{m}})}
\tag{6}
$$

where y_{m} is the dimensionless maximal temperature and $\alpha(v_{\text{sw}}, y_{\text{m}})$ is a correction term due to the finite system length and inhomogeneous boundary conditions; $\alpha \to 0$ and $v_{\text{sw}} \to v_{\infty}$ for an unbounded reactor. The solution of front movement in an unbounded once-through system is quite similar, with[22] $F(y_{\text{m}}) \to (1 - \varepsilon v_{\text{fr}}/v_{\text{o}})^2$. This similarity between the

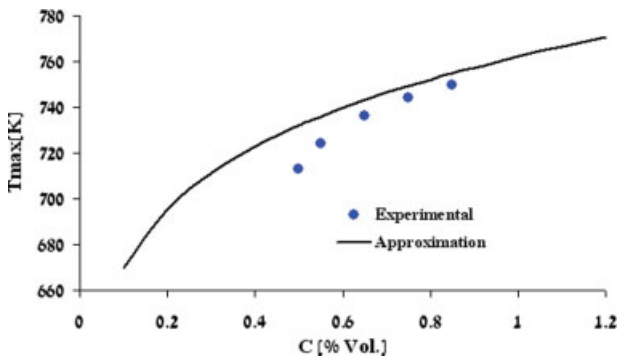

Figure 6. The dependence the measured and approximated maximal temperature on feed concentration (fluid velocity is 0.63 m/s).

[Color figure can be viewed in the online issue, which is available at www.interscience.wiley.com.]

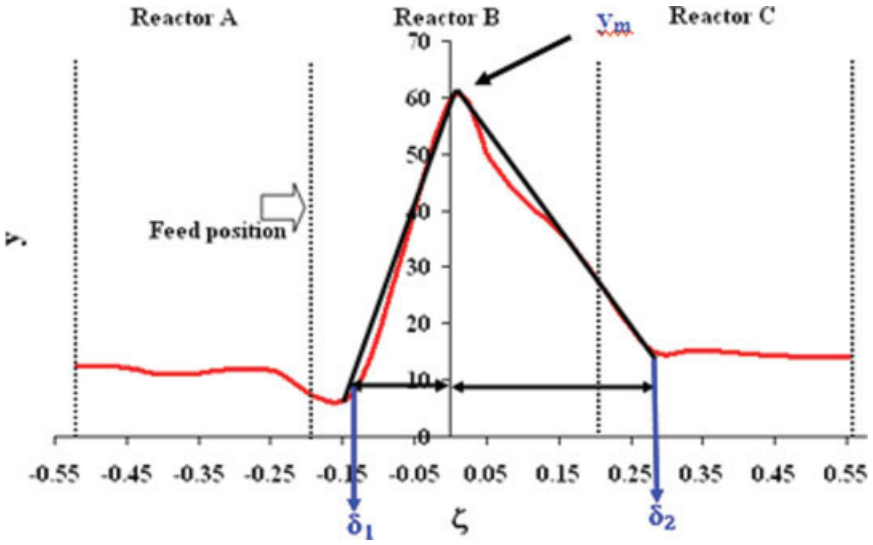

Figure 7. An actual pulse and its triangle-shaped approximation used in the derivation.

[Color figure can be viewed in the online issue, which is available at www.interscience.wiley.com.]

switching velocity (v_{sw}), defined as $v_{sw} = \Delta L/\sigma$, in a long loop reactor and the front velocity (v_{fr}) in an unbounded once-through reactor is expected to hold here as well in the nonadiabatic case. In such a case, it is convenient to transform the governing Eq. 4 using a moving coordinate system with fixed positions of the inlet and outlet:

$$t = t', \quad z' = z - v_{sw}t$$

And, in dimensionless coordinates

$$\tau = \tau', \quad \zeta = \xi - \omega\tau, \quad \omega = \frac{\varepsilon v_{sw}}{v_o}$$

$$\begin{aligned} L_e\frac{\partial y}{\partial \tau'} + (1 - L_e\,\omega)\frac{\partial y}{\partial \zeta} &= \frac{1}{P_{e_y}}\frac{\partial^2 y}{\partial \zeta^2} + BD_aR - W(y - y_w) \\ \frac{\partial x}{\partial \tau'} + (1-\omega)\frac{\partial x}{\partial \zeta} &= D_aR(x,y) \end{aligned} \tag{7}$$

We try to derive such an approximation based on a "steady" frozen front solution ($\partial y/\partial\tau' = \partial x/\partial\tau' = 0$).

In a similarity to an "ideal" front in an adiabatic system, we can define an "ideal" front in a nonadiabatic with the exit temperature $y\ (\zeta \to \infty) = y_w$. For an "ideal" front in an infinitely long system, the boundary condition are modified to

$$\begin{aligned} &\zeta \to -\infty, \quad y \equiv 0 \quad \frac{\partial y}{\partial \zeta} \equiv 0, \quad x \to 0 \\ &\zeta \to +\infty \quad y \equiv y_w \equiv 0 \quad \frac{\partial y}{\partial \zeta} \equiv 0 \end{aligned}$$

The mass and heat balances in stationary Eq. 7 can be added as follows:

$$\begin{aligned} (1 - \omega\,\mathrm{Le})\frac{\partial y}{\partial \zeta} &= \frac{1}{P_{e_y}}\partial^2 y/\partial\zeta^2 + B(1-\omega)\frac{\partial x}{\partial \zeta} - Wy \\ (1-\omega)\frac{\partial x}{\partial \zeta} &= D_aR(x,y) \end{aligned} \tag{8}$$

In an adiabatic ($W = 0$) "ideal" front, a simple integration of Eq. 8 allows to obtain a relation between the maximal temperature rise and the front velocity:

$$(1 - \omega\mathrm{Le})y_m = B(1-\omega)x_m.$$

In the nonadiabatic case, the temperature profile is assumed, for simplicity, to be linear at the pulse front ($-\delta_1 < \xi < 0$) and at its back ($0 < \xi < \delta_2$) (Figure 7). To estimate the effect of the heat loses, we integrate the heat loss in a triangularlike spatial temperature profile (Figure 7) and integrate Eq. 8 (from $-\infty$ up to 0) to find

$$\begin{aligned} -\infty < \zeta < 0 \Rightarrow 0 &= (1 - \mathrm{Le}\ \omega)y_m - B(1-\omega)x_m + \frac{Wy_m\delta_1}{2} \\ 0 < \zeta < \infty \Rightarrow 0 &= -(1 - \mathrm{Le}\ \omega)y_m + \frac{Wy_m\delta_2}{2} \end{aligned} \tag{9}$$

and with δ_1 to be determined later from experimental results. Equation 9 for $\zeta < 0$ can be written as

$$y_m = \frac{B(1-\omega)x_m}{(1 + \frac{W\delta_1}{2} - \mathrm{Le}\ \omega)} \tag{10}$$

An inspection of Eq. 7 shows that $\omega < 1$ (otherwise $\partial x/\partial\zeta < 0$). To ensure that $y_m > 0$, the dimensionless heat front velocity must obey $Le\ \omega < (1 + W\delta_1/2)$.

Equation 10 provides relation between ω and y_m: ω cannot be determined, as the value of y_m is unknown. To calculate ω, let us integrate Eqs. 8 under certain simplifying assumption.

$$\begin{aligned} \partial y/\partial\zeta = P_{e_y}\frac{(1-\omega)B}{y_m}y - yP_{e_y}\frac{W\delta_1}{2} \\ - P_{e_y}\frac{y_mW\delta_1}{2} - P_{e_y}B(1-\omega)x + P_{e_y}W\int_{\zeta}^{0} y\,d\zeta \end{aligned} \tag{11}$$

We shall use the extrapolation method developed by Kiselev (1993). As is shown in the Appendix, the main impact of various

terms can be estimated by their values around the front position. To simplify the problem, we can replace the last term of Eq. 11 by its approximation, $P_{ey}Wy_m\delta_1$.

In Appendix, we show (Eqs. A7) that the pulse velocity is

$$\omega = 1 - \frac{(\gamma + y_m)}{\gamma}\sqrt{\frac{D_a K(y_m)}{P_{e_y} B}} \quad K(y_m) = \exp\left(\frac{\gamma y_m}{\gamma + y_m}\right) \quad (12)$$

Substituting ω from Eq. 10 into Eq. 12, we obtain an equation with respect to a single unknown variable y_m:

$$\frac{D_a}{P_{e_y} B}\left(1 + \frac{y_m}{\gamma}\right)^2 \exp\left(\frac{\gamma y_m}{\gamma + y_m}\right) = \frac{y_m^2\left(1 + \frac{W\delta_1}{2} - \mathrm{Le}\right)^2}{\left(B - y_m \mathrm{Le}\right)^2} \quad (13)$$

In adiabatic system ($W \to 0$), we obtain

$$\frac{D_a}{P_{e_y} B}\left(1 + \frac{y_m}{\gamma}\right)^2 \exp\left(\frac{\gamma y_m}{\gamma + y_m}\right) = \frac{y_m^2(1 - \mathrm{Le})^2}{\left(B - y_m \mathrm{Le}\right)^2} \quad (14)$$

which for $\mathrm{Le} \gg 1$ and $y_m\,\mathrm{Le} \gg B$ is reduced to

$$F(y_m) = \frac{D_a}{P_{e_y} B}\left(1 + \frac{y_m}{\gamma}\right)^2 \exp\left(\frac{\gamma y_m}{\gamma + y_m}\right) = 1 \quad (15)$$

which agrees with solutions in the literature (Eq. 6)

Gattica et al.[20] developed an approximation for maximal temperature and front velocity using similar assumptions as well as assuming that the reaction zone is extremely narrow:

$$y_m = \frac{B(1 - \omega)}{\left((1 - \mathrm{Le}\ \omega)^2 + \frac{4W}{\mathrm{Pe}_y}\right)^{1/2}}$$
$$\omega = 1 - \left(\frac{y_m + \gamma}{\gamma}\right)\sqrt{\frac{D_a K(y_m)}{\mathrm{Pe}_y B}} \quad (16)$$

When comparing our approximation, which uses an experimentally determined value of pulse width (δ_1) with theirs, we find that δ_1 should be

$$\delta_1 = W(\mathrm{Le}\ \omega - 1)\left[1 - \sqrt{1 + \frac{4W}{\mathrm{Pe}_y(1 - \mathrm{Le}\ \omega)^2}}\right] \quad (17)$$

Using the experimental values, we find $\delta_1 \sim 10^{-3}$ vs. $\delta_1 \sim 10^{-1}$ determined from Figure 7; therefore, in this work, an alternative approximation was developed.

Application

We use Eq. 13, using the experimentally determined value of δ_1 (Figure 7) to predict the maximal temperature and the pulse velocity.

As the discussion at the end of the previous chapter shows, the procedure describes well the experimental observations in Figures 5 and 6.

Conclusions

A system of loop-shaped reactor network was experimentally investigated as an alternative to the reverse-flow reactor. The system including three reactors, each with an inert section, with feedback control of feed position has been successfully operated for ethylene oxidation. The system can be controlled by a simple set of two switches activated by crossing two temperature set points. This strategy serves for startup and is stable with respect to fluctuating inlet concentrations and also of gas flow rates. Increasing feed flow rate and feed ethylene concentration were found to lead to higher front velocities and reactor maximal temperatures. An analytical approximation for the heat front velocity and the maximal reactor temperature in a nonadiabatic system has been developed. The experimental results are in a good agreement with the derived analytical approximations.

The loop reactor may admit higher temperatures than those of the RF reactor, and, when deactivation cannot be avoided, it spreads evenly around the system. Yet, the loop reactor requires more valves and a feedback control. This work shows that the latter obstacles can be overcome.

Acknowledgments

MS is a member of the Minerva Center of Nonlinear Dynamics. ON is partially supported by the Center for Absorption in Science, Ministry of Immigrant Absorption State of Israel. We acknowledge the innovative valve design suggested by our Machine Shop, headed by Mr. M. Cohen and by the Faculty Engineer Mr. E. Perlov.

Notation

Symbols

A = pre-exponentional factor (s^{-1})
B = dimensionless temperature rise in adiabatic model
C = concentration (gmol m^{-3})
Cp_f = gas heat capacity (kJ kg^{-1} K^{-1})
Cp_s = solid heat capacity (kJ kg^{-1} K^{-1})
d = reactor diameter (m)
D = effective axial mass dispersion (m^2 s^{-1})
Da = Damkohler number
E_a = activation energy (kJ $gmol^{-1}$)
k_s = solid thermal conductivity (kJ m^{-1} s^{-1} K^{-1})
K = another dimensionless reaction (m^3 $gmol^{-1}$)
L = reactor length (m)
Le = Lewis number in adiabatic model
Pe_y = Peclet number for heat in adiabatic model
r = reaction rate (gmol s^{-1})
R = dimensionless reaction rate
R_g = gas constant (8.314 kJ $kmol^{-1}$ K^{-1})
t = time (s)
t' = time in a moving coordinate (s)
T = temperature (K)
T_{in} = inlet temperature (K)
T_{ign} = ignition temperature (K)
T_m = maximal temperature (K)
T_{sw} = switch temperature (K)
T_w = wall temperature (K)
U = heat transfer coefficient (kJ m^{-2} s^{-1} K^{-1})
W = dimensionless heat transfer coefficient
v_o = gas velocity
v_{fr} = heat front velocity (s)
v_{sw} = switch velocity (s)
w = another dimensionless temperature
x = conversion
x_m = maximal conversion
y = dimensionless temperature
y_m = dimensionless maximal temperature
y_w = dimensionless wall temperature

z = axial coordinate (m)
z' = axial coordinate in a moving coordinate (m)
$-\Delta H$ = heat of combustion (kJ gmol^{-1})

Greek letters

γ = dimensionless activation energy
ΔT_{ad} = adiabatic temperature rise (K)
ε = reactor bed void fraction
σ = switching period (s)
ξ = dimensionless axial coordinate
ρ_g = gas density (kg m^{-3})
ρ_s = solid density kg m^{-3}
τ = dimensionless time
τ' = dimensionless time in a moving coordinate
ω = dimensionless front velocity
ζ = dimensionless axial coordinate in a moving coordinate

Abbreviations

CCR = counter-current reactor
LR = loop reactor or ring reactor
RF = reverse flow
VOC = volatile organic compounds

Literature Cited

1. Ben-Tullilah M, Alajem E, Gal R, Sheintuch M. Flow-rate effects in flow-reversal reactors: experiments, simulations and approximations. *Chem Eng Sci*. 2003;58:1135–1146.
2. Matros YuSh, Bunimovich GA, Noskov AS. The decontamination of gases by unsteady-state catalytic method: theory and practice. *Catal Today*. 1993;17:261–273.
3. Brinkmann M, Barresi AA, Vanni M, Baldi G. Unsteady state treatment of very lean waste gases in a network of catalytic burners. *Catal Today*. 1999;47:263–277.
4. Sheintuch M, Nekhamkina O. The asymptotes of loop reactors. *AIChE J*. 2005;51:224–234.
5. Lauschke G, Gilles ED. Circulating reaction zones in a packed-bed loop reactor. *Chem Eng Sci*. 1994;49:5359–5375.
6. Noskov AS, Bobrova LN, Matros YuSh, Reverse-process for NOx-Off gases decontamination. *Catal Today*. 1993;17:293–300.
7. Eigenberger G, Nieken U. Catalytic combustion with periodic flow reversal. *Chem Eng Sci*. 1988;43:2109–2115.
8. Kolios G, Frauhammer J, Eigenberger G. Autothermal fixed-bed reactors concepts. *Chem Eng Sci*. 2000;55:5945–5967.
9. Boreskov GK, Matros YuSh, Kiselev OV. Catalytic processes under nonsteady-state conditions. I. Thermal front in the immobile catalyst layer. *Kinet Catal*. 1979;20:773–780.
10. Boreskov GK, Matros YuSh. Unsteady state performance of heterogeneous catalytic reactions. *Catal Rev Sci Eng*. 1983;25:551–590.
11. Matros YuSh. *Catalytic Processes Under Unsteady-State Conditions*. Amsterdam: Elsevier, 1989.
12. Gerasev AP, Matros YuSh. Nonsteady-state process for ammonia synthesis. *Teoreticheskie Osnovy Khimicheskoi Tekhnol*. 1991;25:821–827.
13. Van den Bussche KM, Froment GF. The STAR configuration for methanol synthesis in reversed flow reactors. *Can J Chem Eng*. 1996;74:729–734.
14. Nekhamkina O, Sheintuch M. Approximate design of loop reactors. *Chem Eng Sci*. In press.
15. van de Beld L, Westerterp KR. Operation of a catalytic reverse flow reactor for the purification of air contaminated with volatile organic compounds. *Can J Chem Eng*. 1997;75:975–983.
16. Nussbaumer T, Wakili GK, Tanner Ch. Experimental and numerical investigation of the thermal performance of a protected vacuum insulation system applied to a concrete wall. *Appl Energy*. 2005;83:841–855.
17. Wei-Han T, Wen-Fa S, Jian-Yuan L. Development of vacuum insulation panel *J Cell Plast*. 1997;33:545–556.
18. Barresi AA, Fissore D. Comparison between the reverse flow and a network of reactors for the oxidation of lean VOC mixture. *Chem Eng Technol*. 2002;25:421–426.
19. Mandler J, Lavie R, Sheintuch M. An automated catalytic system for the sequential optimal discrimination between rival model. *Chem Eng Sci*. 1983;38:979–990.
20. Gattica JE, Puszynski J, Hlavacek V. Reaction front propagation in nonadiabatic exothermic reaction flow system. *AIChE J*. 1987;33:819–833.
21. Frank-Kamenetski DA. *Diffusion and Heat Exchange in Chemical Kinetics*. Princeton, NJ: Princeton University Press, 1955.
22. Kiselev OV. *Theoretical study of the phenomena of heat waves movement in catalytic bed (in Russian)*. Novosibirsk, Russia: Russian Academy of Sciences, Institute of Catalysis, 1993.

Appendix

We follow the procedure of Kiselev[22] to determine the maximal temperature: introducing a new variable $w = y/y_m$, Eq. 12 in text can be rewritten as

$$\frac{\partial w}{\partial \zeta} = \frac{P_{e_y} B}{y_m}(1-\omega)\left[(w-x) - w\frac{y_m W \delta_1}{2B(1-\omega)}\right]$$
$$(1-\omega)\frac{\partial x}{\partial \zeta} = D_a R \qquad \text{(A1)}$$
$$\frac{y_m W \delta_1}{2B(1-\omega)} = Q, \quad K(y_m) = \exp\left(\frac{\gamma y_m}{\gamma + y_m}\right)$$

Dividing the two equations mentioned earlier, we obtain

$$\frac{\partial x}{\partial w} = \frac{y_m D_a K (1-x)}{P_{e_y} B (1-\omega)^2 [w(1-Q) - x]} \qquad \text{(A2)}$$

Assuming full conversions ($x_m = 1$) at the pulse (peak), we obtain

$$\frac{\partial x}{\partial w} = f(w,x) = p(w) g(w,x),$$
$$p(w) = \frac{y_m D_a K}{P_{e_y} B (1-\omega)^2}, \quad g(w,x) = \frac{(1-x)}{w(1-Q) - x} \qquad \text{(A3)}$$

Note that $g(w,x)$ possesses a singularity if $x \to 1$ while $w \to 1$ and $0 < Q \ll 1$; however, the limits $g(w,x)$ and dx/dw (x'_w) are finite

$$\lim_{w,x\to 1} x'_w = \lim f(w,x) = p(1)\frac{-x'_w}{1-x'_w}$$
$$\lim_{w,x\to 1} x'_w = 1 + P(1) \qquad \text{(A4)}$$

Integrating Eq. A2, we obtain

$$1 = \int_0^1 p(w) g(w,x) dw \qquad \text{(A5)}$$

Using the assumption of a narrow reaction zone, the integral in (A5) can be approximated as

$$x(w) = 1 - x'_w(1-w)$$

and substitute in (A3)

$$g(w,x) \cong \frac{x'_w(1-w)}{w-1+x'_w(1-w)}$$

Using now (A4)

$$g(w,x) \cong \frac{1+P(1)}{1+P(1)-1} = 1 + \frac{1}{P(1)} \cong 1$$

Here, we assume that $P(1) \gg 1$.[22] Substituting $g(w,x)$ into Eq. A5, we obtain $\int_0^1 p(w)dw = 1$ or

$$\frac{y_m D_a}{P_{e_y} B(1-\omega)^2} \int_0^1 \exp\left[\frac{\gamma(wy_m)}{\gamma + wy_m}\right] dw = 1 \qquad \text{(A6)}$$

Equation 11 for a closed system with respect to the two unknown (ω and y_m). The integral in Eq. A5 can be estimated using the Frank-Kamenetski[21] approach. Consider the power in the area of $w = 1$:

$$\left.\frac{\gamma(wy_m)}{\gamma + wy_m}\right|_{w\to 1} \cong \frac{\gamma y_m}{\gamma + y_m} + \left.\frac{\gamma y_m(\gamma + wy_m) - \gamma y_m^2}{(\gamma + y_m)^2}\right|_{w=1} (w-1) + o((w-1)^2)$$

$$\left.\frac{\gamma(wy_m)}{\gamma + wy_m}\right|_{w\to 1} = \frac{\gamma y_m}{\gamma + y_m} + \frac{\gamma^2 y_m (w-1)}{(\gamma + y_m)^2}$$

Now the integral in the LHS of Eq. A5 is

$$\int_0^1 p(w)du \cong \frac{y_m D_a}{P_{e_y} B(1-\omega)^2} \exp\frac{\gamma y_m}{\gamma + y_m} \int_0^1 \exp\frac{\gamma^2 y_m (w-1)}{(\gamma + y_m)^2} dw$$

$$= \frac{D_a(\gamma + y_m)^2 K(y_m)}{\gamma^2 P_{e_y} B(1-\omega)^2} \left[1 - \exp\frac{-\gamma^2 y_m}{(\gamma + y_m)^2}\right] \cong \frac{D_a(\gamma + y_m)^2 K(y_m)}{\gamma^2 P_{e_y} B(1-\omega)^2}$$

As the last term in the square brackets can be neglected in comparison with one. Equation 25 can be reduced to the following algebraic equation:

$$\frac{D_a(\gamma + y_m)^2 K(y_m)}{\gamma^2 P_{e_y} B(1-\omega)^2} = 1 \qquad K(y_m) = \exp\left(\frac{\gamma y_m}{\gamma + y_m}\right) \qquad \text{(A7)}$$

Manuscript received Nov. 6, 2007, and revision received May 1, 2008.